Inferential framework for nonstationary dynamics. II: Application to a model of physiological signaling

Andrea Duggento[1], Dmitri G. Luchinsky[1,2,3], Vadim N. Smelyanskiy[2], Igor Khovanov[1,*] and Peter V. E. McClintock[1]
[1] *Department of Physics, Lancaster University, Lancaster LA1 4YB, UK*
[2] *NASA Ames Research Center, Mail Stop 269-2, Moffett Field, CA 94035, USA and*
[3] *Mission Critical Technologies Inc., 2041 Rosecrans Ave. Suite 225 El Segundo, CA 90245*

The problem of how to reconstruct the parameters of a stochastic nonlinear dynamical system when these are time-varying is considered in the context of online decoding of physiological information from neuron signaling activity. To model the spiking of neurons, a set of FitzHugh-Nagumo (FHN) oscillators is used. It is assumed that only a fast dynamical variable can be detected for each neuron, and that the monitored signals are mixed by an unknown measurement matrix. The Bayesian framework introduced in Paper I (Phys. Rev. E **77**, 06110500 (2008)) is applied both for reconstruction of the model parameters and elements of the measurement matrix, and for inference of the time-varying parameters in the non-stationary system. It is shown that the proposed approach is able to reconstruct unmeasured (hidden) slow variables of the FHN oscillators, to learn to model each individual neuron, and to track continuous, random and step-wise variations of the control parameter for each neuron in real time.

PACS numbers: 02.50.Tt, 05.45.Tp, 05.10.Gg, 05.45.Xt

I. INTRODUCTION

Time variability and nonlinearity are natural ingredients of physiological systems. In addition, a system's environment and its own internal complexity often creates a strong fluctuational background which is frequently an essential feature of the dynamics. It is a context where physiological models are rarely known from the first principles, and model identification and parameter inference become indispensable from the points of view of both fundamental and applied physiology [1, 2] and in a view of likely medical applications. In many situations the real-time tracking of physiological parameters is the key to successful applications including e.g. brain-controlled interfaces [3, 4]. However, the interplay of noise, nonlinearity, and the time-variability of the model parameters makes it difficult to extract reliable information from the data, and very difficult to do so quickly. Accordingly, the simplifying assumptions of linearity and/or determinism [2, 5] are frequently made in an attempt to facilitate inference rather than on physiological grounds.

In addition, physiologically important parameters that describe specific features of the system state or system dynamics are not usually directly measurable and have to be inferred from measurements of other types of information. At present there are no general methods available to solve this problem if the model is stochastic, nonlinear and non-stationary, i.e. its parameters vary in time.

In Paper I [6], we introduced a general Bayesian framework that allows one to identify a nonlinear stochastic model from time-series data and to infer its time-varying parameters in real time. In the present paper we verify the approach by applying it to the analysis of a model of physiological signalling. The model chosen is a set of the FitzHugh-Nagumo (FHN) systems [7–9]. It has been found useful in analyzing dynamics of nerve fibres [10] and certain muscle cells in heart tissue [11–13]. It has also been used intensively in studies of passive myelinated axons [14] and various forms of arrythmia and cardiac activation evolution [15]. The control of such neural-related dynamics is important in the context of bio-technological applications ranging from neural models of voluntary movement[16] to studies of control in nerve conduction[17].

In our model, the measured signals corresponding to fast variables of the FHN system (e.g. action potentials), are mixed by the unknown measurement matrix. Slow variables are hidden, which is the case in most real applications. It is assumed that physiological information is coded in the time-varying control parameters η of each FHN system. Our goals will be to reconstruct the hidden variables and the measurement matrix, to learn the parameters of each individual system, and to use this information for extracting the time-variation of the control parameter η in real time. We will show, in particular, that the approach is able to decode large stepwise changes, as well as random and continuous variations of the control parameter, for each oscillator in real time. Furthermore, we will show that the parameter-tracking algorithm can effectively be embedded into the inferential learning framework, enabling us to reconstruct both the unmeasured (hidden) variables of the FHN oscillators and the model parameters. For simplicity, we will assume that FHN systems are not coupled and that the dynamical equation for the slow variable does not include a random force. However, both coupling and noise in the hidden variables can very easily be incorporated into the method, as will be shown elsewhere.

The paper is organized as follows. In Sec. II a model of FHN systems coupled by unknown measurement matrix

*Electronic address: i.khovanov@warwick.ac.uk

is presented and then reduced to standard form suitable for analysis within the Bayesian framework. Convergence of the model parameters for the case of stationary signals is discussed in Sec. III. Their convergence and online tracking when the system is non-stationary are presented in Sec. IV. Finally, the results obtained are summarized and conclusions are drawn in Sec. V.

II. SYSTEM OF FITZHUGH-NAGUMO OSCILLATORS

In a typical physiological situation neurons fire at the rate of ∼5-10 s^{-1}. The correlation time of the control parameter is ∼500-1000 ms. The correlation times of other model parameters in the non-stationary case are ∼5 s. A typical sampling rate for measurements is ∼20 kHz. In order to follow the time-variations, it is necessary for the computation time to be less than the shortest characteristic time in the system, i.e. that for variation of the control parameters. So we must aim for a computational inference delay time of less than 500 ms.

To model this spiking activity we use the well-known FitzHugh-Nagumo system in the form

$$\begin{aligned} \dot{v}_j &= -v_j\,(v_j-\alpha_j)\,(v_j-1) - q_j + \eta_j + \sqrt{D_{ij}}\,\xi_j, \\ \dot{q}_j &= -\beta\, q_j + \gamma_j\; v_j, \\ \langle \xi_j(t)\,\xi_i(t')\rangle &= \delta_{i\,j}\,\delta(t-t'), \quad j=1:L. \end{aligned} \tag{1}$$

This system (1) represents the simplified dynamics of L non-interacting neurons [8], where v_j model the membrane potentials and q_j are slow recovery variables. Fig 1 illustrates the dynamics for one oscillator in absence of noise; values of the other parameters are α=0.4, η=0.3; β=0.0151; γ=0.0153.

We assume that the important physiological information is encoded in the parameter η, which controls the frequency of firing. In practice, this information is difficult to extract because signals collected from biological systems are noisy and often mixed with an unknown measurement matrix. To analyze the situation in a realistic way we introduce dynamical noise into the model system (1) and a measurement matrix X into the following measurement model

$$y_i \;=\; X_{ij}\, v_j\,. \tag{2}$$

Here y_i are measured variables, related to v_j by linear transformation with the *unknown* matrix X. An example of noisy signals before and after the mixing are shown in the Fig. 2. We suppose that the only accessible information is contained in y_i. The problem is therefore to learn the model parameters $\mathcal{M} = \{\eta_i, \alpha_i, q_i(0), \gamma_i, D_{ij}, X_{ij}\}$ from the time series data $\{y_i\}$, and to use this information for fast on-line tracking of the time-varying parameters $\{\eta_i\}$ for each neuron. It was shown in I that this problem can be treated within a general inferential framework by

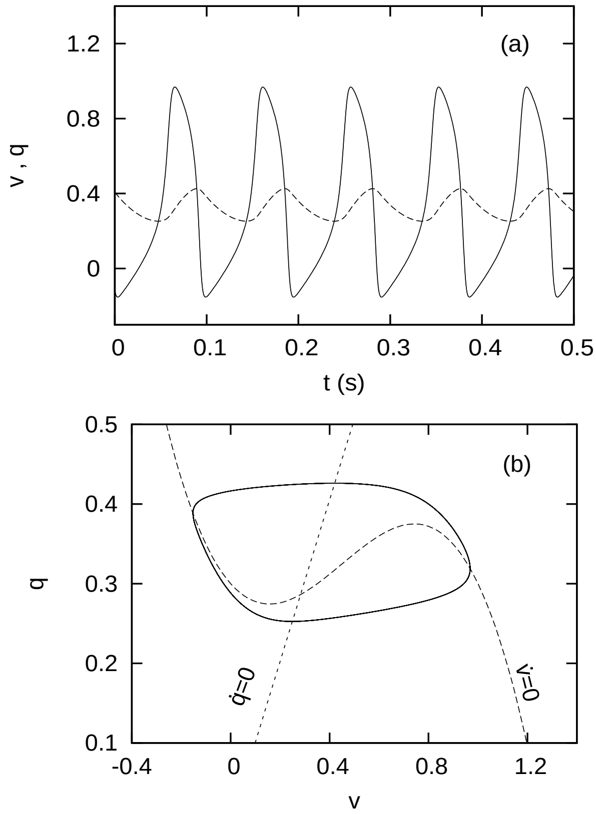

Figure 1: Numerical simulation of the FitzHugh-Nagumo oscillator (1). (a) Examples of the time-traces of v_j (solid line) and q_j (dashed line). (b) Nullclines are shown by the dashed (1st equation) and dotted (2nd equation) lines, and the corresponding phase trajectory is shown by the thin solid line.

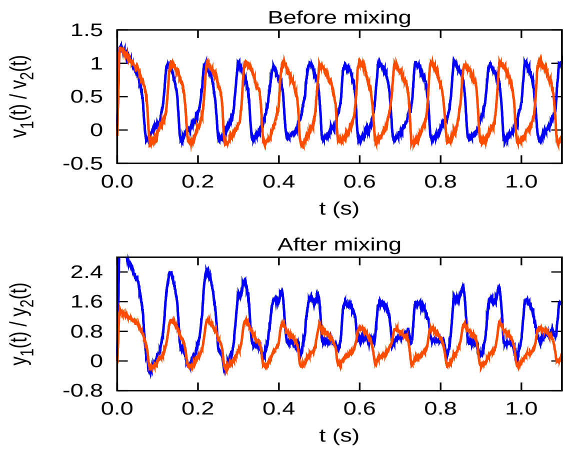

Figure 2: (Color online) Time-series data generated by the model (1), (2) before and after mixing, for the parameters given in Table I. Parameters η_1 and η_2 fluctuate between 0.35 and 0.45. The blue solid lines show $v_1(t)$ and $y_1(t)$, and the red dotted lines show $v_2(t)$ and $y_2(t)$.

integrating the middle set of equations in (1) to obtain

$$q_j(t) = \gamma \int_0^t d\tau e^{-\beta\,(t-\tau)} v_j(\tau) + e^{-\beta\,t} q_j(0). \quad (3)$$

On substituting (3) into the top equation in (1) we have

$$\begin{aligned} \dot{v}_j &= -\alpha_j v_j + (1+\alpha_j) v_j^2 - v_j^3 + \eta_j \\ &- \gamma_j \int_0^t d\tau e^{-\beta\,(t-\tau)} v_j(\tau) - e^{-\beta\,t} q_j(0) + \sqrt{D_{ij}}\xi_j. \end{aligned} \quad (4)$$

Here $j = 1, ..., L$, and $q_j(0)$ is a set of initial coordinates for the unobservable variable $q_j(t)$. Thus the reconstruction of unobservable variables $q_j(t)$ is reduced to the inference of the L initial conditions $q_j(0)$.

Furthermore, the variables $v_j(t)$ can also be excluded from further consideration by using Eq. (2). On substituting $\boldsymbol{v} = \boldsymbol{X}^{-1}\boldsymbol{y}$ into (4) we obtain in vector notation:

$$\begin{aligned} \dot{\boldsymbol{y}} = \boldsymbol{X}\boldsymbol{\alpha}\left(\boldsymbol{X}^{-1}\,\boldsymbol{y}\right) + \boldsymbol{X}(1+\boldsymbol{\alpha})\left(\boldsymbol{X}^{-1}\,\boldsymbol{y}\right)^2 + \\ \boldsymbol{X}\left(\boldsymbol{X}^{-1}\,\boldsymbol{y}\right)^3 + e^{-\beta\,t}\boldsymbol{X}\boldsymbol{q}_0 - \\ \int_0^t e^{\beta(t-\tau)}\boldsymbol{X}\boldsymbol{\gamma}\left(\boldsymbol{X}^{-1}\,\boldsymbol{y}\right)d\tau + \boldsymbol{X}\boldsymbol{\eta} + \boldsymbol{X}\sqrt{\boldsymbol{D}}\boldsymbol{\xi}(t), \end{aligned} \quad (5)$$

where $q_0 = q(t=0)$, $\boldsymbol{\alpha}$ and $\boldsymbol{\gamma}$ are matrices with α_i and γ_i on respective diagonals, and

$$\left(\boldsymbol{X}^{-1}\,\boldsymbol{y}\right)^n = \begin{pmatrix} \left(\sum_{i=1}^{L} x_{1i} y_i\right)^n & \dots & 0 \\ \vdots & \ddots & \vdots \\ 0 & \dots & \left(\sum_{i=1}^{L} x_{Li} y_i\right)^n \end{pmatrix}.$$

Here x_{ji} are elements of the inverse matrix $\boldsymbol{X}^{-1}$.

The advantage of the presentation (5) is that it allows for the fastest on-line tracking of the control parameters of the system (1) in the case of small measurement noise. In what follows we demonstrate this point using as an example a system of two FHN oscillators. However, the results reported below can be readily extended to a set of L linearly-coupled FHN systems. We will refer to system (5) as "transformed dynamics" to distinguish it from the "reduced dynamics" of (4).

$\alpha_1 = 0.35$	$\eta_1 = 0.4$
$\alpha_2 = 0.20$	$\eta_2 = 0.3$
$\gamma_1 = 0.0153$	$\beta = 0.0151$
$\gamma_2 = 0.0153$	
$d_{11}= 0.0002$	$d_{12}= 0.00007$
$d_{22}= 0.0002$	$d_{21}= 0.00007$
$x_{11}= 1.7$	$x_{12}= 0.8$
$x_{22}= 0.2$	$x_{21}= 0.9$

Table I: Parameter values of the model (1), (2) used to generate stationary time-series data.

III. STATIONARY DYNAMICS AND CONVERGENCE

To infer the parameters of the system of L FHN oscillators (5) within the stationary regime we introduce the following base functions

$$\begin{aligned} \phi(x) = \{&\mathbf{1}, y_1, ..., y_L, y_1^2, y_1 y_2, ..., y_1 y_L, y_2^2, \\ &y_2 y_3, ..., y_2 y_L, ..., y_1^3, y_1^2 y_2, ..., y_1^2 y_L, y_2^3, y_2^2 y_1, ..., \\ &y_2^2 y_L, ..., y_L^2 y_{L-1}\,, y_L^3\,, \Phi_1, ..., \Phi_L\,, e^{-\beta t}\} \end{aligned} \quad (6)$$

where Φ_i is defined as follows

$$\Phi_i \equiv \int_0^t y_i(\tau) e^{\beta(\tau - t)}.$$

The number of base functions,

$$N_\phi = 2 + 2L + \tfrac{L(L+1)}{2} + L^2 \quad (7)$$

increases as L^2 with the number of systems. The number of unknown coefficients of the system (5) is $N_c = N_\phi \times L + L^2 + \frac{L(L+1)}{2}$; it increases as L^3 with the dimension of the system. The first term in N_c is the full set of unknown coefficients, because all possible combinations of the powers of y are included in this set, i.e. it covers the whole model space of the system with polynomial base functions up to power 3. The second term in N_c is the number of unknown elements of the measurement matrix $\boldsymbol{X}$, while the third is the number of the elements of the unknown noise matrix. Only $N_{inf} = N_\phi \times L + \frac{L(L+1)}{2}$ coefficients can be inferred directly from the time series data $\{y_i\}$, and therefore only N_{inf} equations can be formed to find the coefficients of the original system (4) and the elements of the matrix $\boldsymbol{X}$. In practice, however, the number of coefficients of the original system is always significantly smaller then the full set N_{inf}, because of the symmetry that is always present in real systems. In particular, the number of unknown coefficients in the original system (2), (4) is $N_{\mathcal{M}} = 6L + L^2 + \frac{L(L+1)}{2}$ (note that here we have counted coefficients for y_i^2 and y_i^3). I.e. for a system of 2 FHN oscillators we have $N_{inf} = 29$ equations to reconstruct $N_{\mathcal{M}} = 19$ coefficients.

So it should be possible at least in principle to reconstruct all unknown coefficients of the original system for any number of FHN oscillators, provided that we can establish the connection between the set

$$\tilde{\mathcal{M}} = \{\tilde{\eta}_i, \tilde{\alpha}_{ij}, \tilde{b}_{ijk}, \tilde{c}_{ijkl}, \tilde{\gamma}_{ij}, \tilde{q}_{ij}(0), \tilde{D}_{ij}\}$$

of measured variables of the transformed system (5) and the set

$$\mathcal{M} = \{\eta_i, \alpha_i, b_i, c_i, \gamma_i, q_i(0), D_{ij}, X_{ij}\}$$

of unknown parameters of the original reduced dynamics (4), where $b_i = (\alpha_i + 1)$ and $c_i = -1$. Note that coefficients $\tilde{\alpha}_{ij}$, $\tilde{b}_{ijk}$, $\tilde{c}_{ijkl}$, $\tilde{\gamma}_{ij}$ in the expression for $\tilde{\mathcal{M}}$

above correspond to coefficients A_{ij}, B_{ijk}, C_{ijkl}, Γ_{ij} in Eqs. (36), (37) of I. In the 2D case the set $\tilde{\mathcal{M}}$ of variables of the transformed dynamics (5) corresponds to the following set of the base functions

$$\begin{aligned}\phi(x) = \{\mathbf{1}\,,\, y_1\,,\, y_2\,,\, y_1^2\,,\, y_2^2\,,\, y_1y_2\,,\, y_1^3\,,\\ y_1^2y_2\,,\, y_1y_2^2\,,\, y_2^3\,,\, \Phi_1\,,\, \Phi_2\,,\, e^{-\beta t}\}.\end{aligned} \tag{8}$$

Once parameters of the transformed dynamics are infered, one has to reconstruct parameters of the original model (1). In general form, the connection between the two sets of coefficients is given by the equations (37)–(39) of paper I. Here we introduce explicit relations for the case $L = 2$.

$$\boldsymbol{X}^{-1}\begin{bmatrix}\eta_1\\ \eta_2\end{bmatrix} = \begin{bmatrix}\tilde{\eta}_1\\ \tilde{\eta}_2\end{bmatrix}, \tag{9}$$

$$\begin{bmatrix}q_{0,1}\\ q_{0,2}\end{bmatrix} = \boldsymbol{X}^{-1}\begin{bmatrix}\tilde{q}_1\\ \tilde{q}_2\end{bmatrix}, \tag{10}$$

$$\begin{bmatrix}\gamma_1 & 0\\ 0 & \gamma_2\end{bmatrix} X^{-1} = \boldsymbol{X}^{-1}\begin{bmatrix}\tilde{\gamma}_{11} & \tilde{\gamma}_{12}\\ \tilde{\gamma}_{21} & \tilde{\gamma}_{22}\end{bmatrix}, \tag{11}$$

$$\begin{bmatrix}\alpha_1 & 0\\ 0 & \alpha_2\end{bmatrix} \boldsymbol{X}^{-1} = \boldsymbol{X}^{-1}\begin{bmatrix}\tilde{\alpha}_{11} & \tilde{\alpha}_{12}\\ \tilde{\alpha}_{21} & \tilde{\alpha}_{22}\end{bmatrix}, \tag{12}$$

$$\tilde{\boldsymbol{D}}\boldsymbol{X}^{-1} = \boldsymbol{X}^{-1}\boldsymbol{D}. \tag{13}$$

The unknown elements x_{ij} of the inverse measurement matrix $\boldsymbol{X}^{-1}$, and the parameters with tildes, are the model parameters of the transformed system (5) that can be inferred directly using time series data $\{y_i\}$. Relations (9)-(13) allow one to reconstruct 15 unknown parameters of the original system, including elements of the noise and measurement matrices. Note, however, that the coefficients $(1+\alpha_i)$ can also be assumed unknown in general and that the following relations can be used to reconstruct them

$$\begin{aligned}\begin{bmatrix}1+\alpha_1 & 0\\ 0 & 1+\alpha_2\end{bmatrix}\begin{bmatrix}x_{11}^2 & 2x_{11}x_{12} & x_{12}^2\\ x_{21}^2 & 2x_{21}x_{22} & x_{22}^2\end{bmatrix}\\ = \boldsymbol{X}^{-1}\begin{bmatrix}\tilde{b}_{111} & \tilde{b}_{112} & \tilde{b}_{122}\\ \tilde{b}_{211} & \tilde{b}_{212} & \tilde{b}_{222}\end{bmatrix},\end{aligned} \tag{14}$$

Similarly, the relationships between the coefficients for polynomials of power 3 are given by

$$\begin{aligned}\begin{bmatrix}-1 & 0\\ 0 & -1\end{bmatrix}\begin{bmatrix}x_{11}^3 & 2x_{11}^2x_{12} & 2x_{11}x_{12}^2 & x_{12}^3\\ x_{21}^3 & 2x_{21}^2x_{22} & 2x_{21}x_{22}^2 & x_{22}^3\end{bmatrix}\\ = \boldsymbol{X}^{-1}\begin{bmatrix}\tilde{c}_{111} & \tilde{c}_{112} & \tilde{c}_{121} & \tilde{c}_{122}\\ \tilde{c}_{211} & \tilde{c}_{212} & \tilde{c}_{221} & \tilde{c}_{222}\end{bmatrix},\end{aligned} \tag{15}$$

Note that in general one could introduce unknown parameters for the coupling between the FHN systems and use relations similar to (12), (14), (15) to reconstruct these parameters. Note also that it is a simple matter to extend equations (9)-(15) to encompass the L-dimensional case.

In the new notation, the 2-dimensional equations for the reduced dynamics take the form

$$\begin{aligned}\dot{y}_i = \tilde{\eta}_i + \tilde{\alpha}_{ij}y_j + \tilde{b}_{ik_1k_2}\, y_{k_1}y_{k_2} + \tilde{c}_{ik_1k_2}\, y_{k_1}y_{k_2}^2\\ + e^{-\beta\, t}\tilde{q}_i - \int_0^t e^{\beta(t-\tau)}\gamma_{ij}\, y_j d\tau + \sqrt{\tilde{D}_{ij}}\xi_j(t),\end{aligned} \tag{16}$$

Equation (16) with $N_\phi = 13$ base functions (8) allows one to apply explicitly the result of paper I to infer the $N_{inf} = 29$ parameters of the transformed system (16). Indeed, the base functions (8) and the model parameters in (16) can be used to factorize the vector field according to Eqs. (7) and (8) of paper I. The minus log-likelihood function and its gradient for the transformed system (16) can then be written using Eqs. (6) and (26) of paper I. As the next step, Eqs. (10-(14) of the main algorithm of paper I can be used to reconstruct the model parameters of the transformed system. Once the parameters of the transformed system have been inferred, one can use Eqs. (9)–(13) to reconstruct the parameters of the original model (1).

In the rest of this section we restrict ourselves to the 2D case and analyze the convergence of the method under stationary conditions. Our goals will be to show the correlation between the convergence of the model parameters and the decay of the eigenvalues $\{\lambda_i\}$ of matrix $\hat{\boldsymbol{\Xi}}^{-1}$ (see I), and to demonstrate how one can speed up the convergence by orders of magnitude by reducing the number of base functions in an appropriate way.

A. Convergence of the parameters of the transformed dynamics

In this section we analyze the convergence of the model parameters of the reduced dynamics (4) as a function of $T = hN$, where h is the sampling time step and N is the number of points in a block of data. The model (1), (2) was integrated using the Heun scheme [18] with the set of parameters shown in Table I. The fast variables of the FHN oscillators $v_1(t)$ and $v_2(t)$ were mixed by the measurement matrix X to generate synthetic time-series data $y_1(t)$ and $y_2(t)$ of measured signal. The latter signals were used as the input for testing the algorithm. An example of the signals $v_1(t), v_2(t)$ and $y_1(t), y_2(t)$ is shown in the Fig. 2.

We now analyze the convergence of the method in the case when all parameters of the reduced model (5), including elements of the measurement matrix are unknown. An example of the convergence of parameters for the reduced model is shown in Fig. 3. The sampling rate was 35 kHz. We used 9 blocks of data with 5000 points

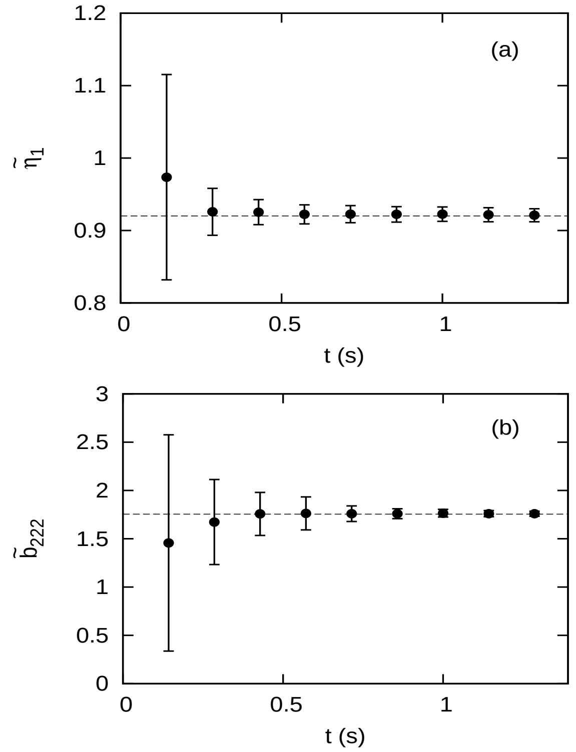

Figure 3: Typical example of the convergence of parameters as a function of signal length. $\tilde{\eta}_1$ and $\tilde{b}_{222}$ are plotted as functions of time, i.e. of the number of data. The first point corresponds to a block of 5000 data points; each successive point after that corresponds to an additional 5000 data, as discussed in the text. Vertical bars show standard deviations of the inferred values, calculated over 1000 realizations. The horizontal dashed lines indicate the true values of the model parameters as given in Tables I and II.

in each block, and these blocks of data were generated at random 1000 times to analyze the statistics of the convergence. The results of the inference are summarized in the Table II. It can be seen that convergence of better then 3.5% is achieved in less than 1 s, even though the coefficients of the highest order polynomials are assumed unknown.

parameter	real	inferred	std. dev.
$\tilde{\eta}_1$	0.9200	0.924384	0.022624
$\tilde{\eta}_2$	0.3500	0.351001	0.009063
$\tilde{b}_{222}$	1.7550	1.758011	0.037047
$\tilde{b}_{112}$	-2.1086	-2.114731	0.068268

Table II: Values of some of the original coefficients inferred using 30000 points. The actual values (second column) are compared with the inferred values (third column), standard deviations are given in the last column.

B. Reconstruction of the mixing matrix

To reconstruct both the mixing matrix X and the parameters of the original system $\mathcal{M}$ from the inferred parameters $\tilde{\mathcal{M}}$ of the transformed system (5), we have to solve equations (9–13) with respect to elements of $\tilde{\mathcal{M}}$. We note that, in the general case of the measurement model, these equations are nonlinear and can be written implicitly as $F_k(\mathcal{M}) = 0, \quad k = 1, ..., K$, where K is the number of equations. In the particular case of transformation given by the simple form of Eqs. (9–13) the solution of this problem can be found by using the standard nonlinear least squares method [19], although an additional optimization over the set of initial values may be required. We stress that the present technique is not restricted to the 2D case and can equally be applied to the general case of N FHN oscillators.

We can now use the inferred parameters of the transformed dynamics (previous subsection, Fig. 3. and Table II) to reconstruct both the elements of the measurement matrix and the model parameters of the original system (4). Examples of convergence of the model parameters are given in the Fig. 4 and Fig. 5, and are summarized in Table III. It can be seen from the table that a relative error of inference of better then 2% is achieved within less then 1 s of measurement time.

parameter	real	inferred	rel. error
X_{11}	1.7	1.686459	0.796526
X_{12}	0.8	0.794263	0.717092
X_{21}	0.2	0.196746	1.626811
X_{22}	0.9	0.898222	0.197610
η_1	0.4	0.406227	1.556788
η_2	0.3	0.302462	0.820660
α_1	-0.35	-0.351992	0.569082
α_2	-0.2	-0.200376	0.188228
b_1	1.35	1.357427	0.550145
b_2	1.2	1.203863	0.321885
c_1	-1.0	-0.999520	0.047957
c_2	-1.0	-0.999114	0.088582

Table III: Values of some of the original coefficients inferred using 30000 points obtained from measurement matrix and real parameters reconstruction. The actual values (second column) are compared with the inferred values (third column), relative errors are given in the last column.

In what follows we will focus on the convergence of the control parameters η and analyze the accuracy and speed of the convergence under various assumptions about time dependence of these parameters and information available about other parameters of the system.

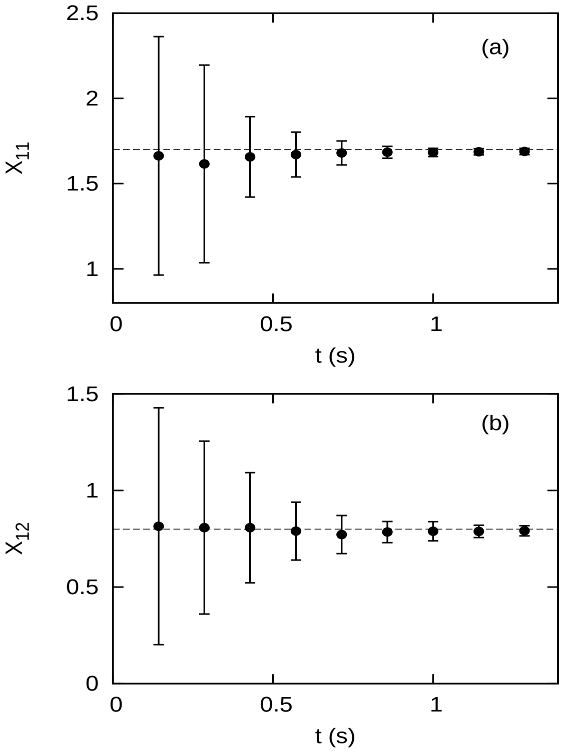

Figure 4: (a) and (b): Typical examples of convergence for two components of the measurement matrix X as a function of the measurement time t. The other model parameters for this numerical test are given in Table I. We have used 9 data blocks with 5000 points in each block. The standard deviations of the inferred parameters shown by the vertical bars are calculated over 1000 realizations. The horizontal lines shows the true values of the model parameters. The sampling rate was 35 kHz.

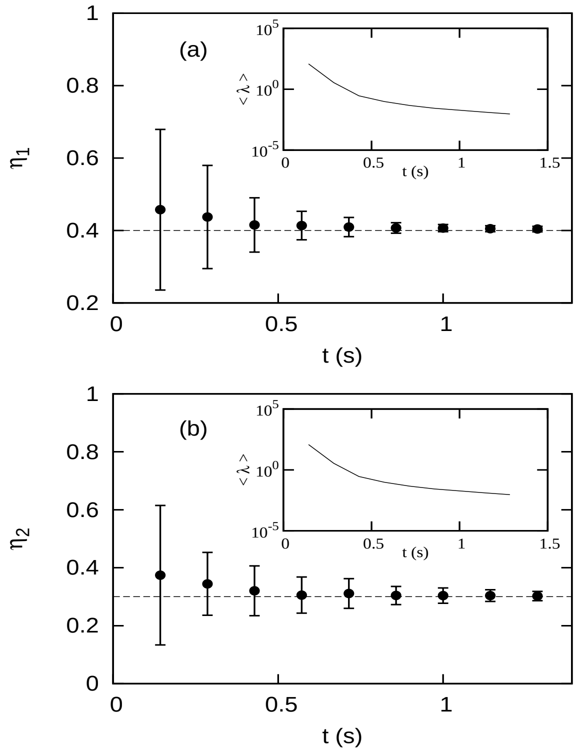

Figure 5: (a) and (b): Convergence of the control parameters η_1 and η_2 as functions of the measurement time t. Values of the other model parameters for this numerical test are given in Table I. We have used 9 data blocks with 5000 points in each block. The standard deviations of the inferred parameters shown by the vertical bars are calculated over 1000 realizations. The horizontal lines show the true values of the control parameters. The sampling rate was 35 kHz. The insets in both figures show the decay of the largest eigenvalues of $\hat{\mathbf{\Xi}}^{-1}$.

C. Convergence speed

We note that to calculate the rate of convergence of model parameters of stochastic nonlinear dynamical systems is, in general, still an open problem. Here we provide a brief discussion, however, based on the results of Sec. C of Paper I [6]. These indicate that the eigenvalues of the matrix $\hat{\mathbf{\Xi}}$ (see Eq. (22) of I) play an important role in the convergence of the model parameters. The meaning of the matrix $\hat{\mathbf{\Xi}}$ is twofold: first, $\hat{\mathbf{\Xi}}$ is the covariance of the posterior density, so it measures directly how sharply peaked this distribution is about its mean value; secondly, $\hat{\mathbf{\Xi}}$ is proportional to $\hat{\mathbf{D}} \otimes \hat{\mathbf{\Phi}}_k^{-1}$ (see Eq. (22) of Paper I), so it is directly influenced by the choice of the base functions and by the correlations between them. It is clear, in particular, that in the case of polynomial base functions the lower the order of polynomials, the smaller will be eigenvalues of $\hat{\mathbf{\Xi}}^{-1}$, and the faster will be their convergence. Indeed, the deviation of the model parameters from their limiting mean values is proportional to a linear combination of the eigenvalues λ_i of $\hat{\mathbf{\Xi}}^{-1}$. So the convergence of the model parameters is determined by the the values and decay rates of the largest eigenvalues of $\hat{\mathbf{\Xi}}^{-1}$. The latter in turn depends on the *a priori* information available about the model parameters. For the polynomial base functions, which is the case of transformed dynamics (5), the most important information from the point of view of convergence speed is knowledge of the coefficients for the polynomials of higher order.

To illustrate this point we calculate the eigenvalues of $\hat{\mathbf{\Xi}}^{-1}$ under various assumption about the number of known parameters in the model. The results of this analysis are shown in the Fig. 6. It can be seen from the figure that when no information is available about model parameters (i.e. all the parameters are unknown) the largest eigenvalue of $\hat{\mathbf{\Xi}}^{-1}$ has an initial value of the order 10^2 and decays to 10^{-2} over a measurement time $t = 1.3$ sec. The correlation between the decay of the largest eigenvalue and the convergence of the η parameters in this case is evident from the Fig. 5. When the coefficients of the cubic and quadratic terms in system (4) are known, the value of the largest λ_i of $\hat{\mathbf{\Xi}}^{-1}$ (shown by the blue dashed line in Fig. 6) is reduced by three orders

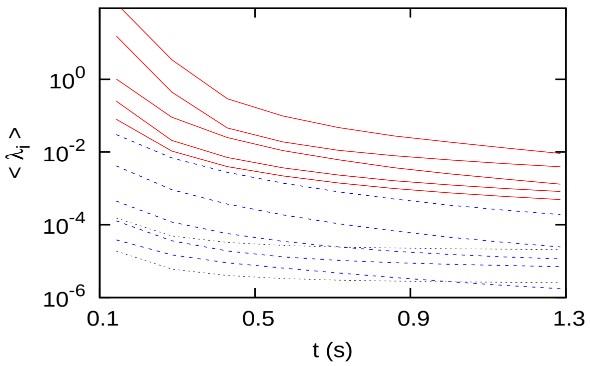

Figure 6: (Color online) The largest eigenvalues λ_i of the matrix $\hat{\boldsymbol{\Xi}}^{-1}$ under different assumptions: (i) when none of the coefficients of the dynamics in eq.(4) are known (full red lines); (ii) when the coefficients of the third and second powers are known (dashed blue lines); (iii) when all parameters except η_i are known (dotted black lines). The dynamical coefficients are the same as in Fig. 4. The number of runs to obtain the averaged convergence was 1000 for each data block size. The actual distribution for each eigenvalue is highly asymmetric over the number of the runs, and typical values of λ_i are lower than their respective means.

of magnitude. When all parameters of the system (4) are known except the control parameters η, the largest value of λ_i of $\hat{\boldsymbol{\Xi}}^{-1}$ (shown by the black dotted lines in Fig. 6) is further reduced by two orders of magnitude.

In the latter case convergence of the inferred parameters η_i to their true values is much faster. To verify this point the following test was performed: (i) first a signal of length 1 s was generated with stationary dynamics and used to infer all the model parameters; (ii) next, the parameters η_i were changed in a step-like manner; and (iii) the convergence of the inferred parameters η_i was analyzed as a function of the length of the step. The results are shown in Fig. 7 It is evident that the time scale for the convergence of η is ~ 20 ms as compared to the convergence over ~ 1 s in Fig. 6. It is therefore clear that the computational delay time of < 500 ms desired for physiological applications can be easily achieved within our Bayesian framework. Next, we consider the efficiency of the method under non-stationary conditions.

IV. NON-STATIONARY DYNAMICS

We consider the situation when all parameters except η_i (4) are fixed at the values given in Table I, but the control parameters η_i are allowed to change, either stepwise or continuously.

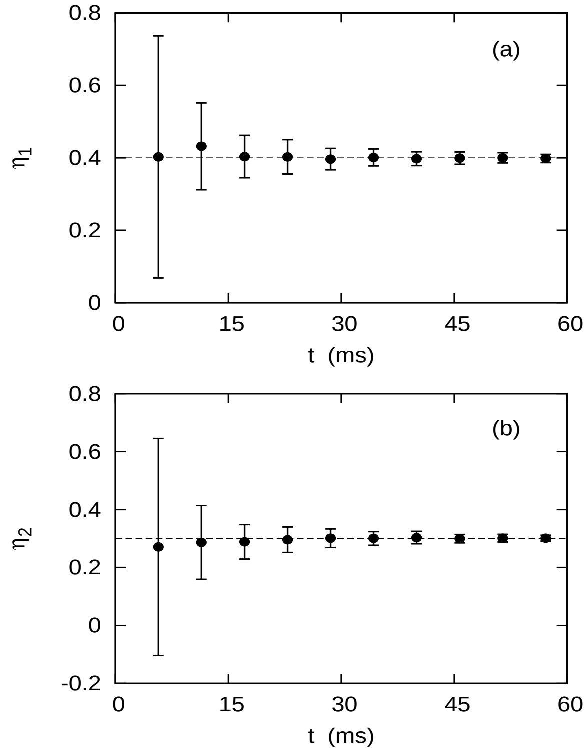

Figure 7: Typical example of the fast convergence of the control parameters (a) η_1 and (b) η_2, as functions of time (length of signal). The first point corresponds to 200 data points in one block. For each next point the number of data points was increased by 200. The vertical lines show the standard deviations of the inferred values of the control parameters calculated over 1000 runs. The horizontal dashed lines indicate the true values of the parameters. Mixing matrix is $\begin{smallmatrix} 1.7 & .8 \\ .2 & .9 \end{smallmatrix}$. The inferred parameters η_i starts from an initial value of $\eta_1 = \eta_2 = 0.2$ and converge quickly to the true values of $\eta_1 = 0.4, \eta_2 = 0.3$. The coefficient α_i,β_i ,γ_i and d_{ij} are given in Table I. The noise amplitude is $\sqrt{d_1} = \sqrt{d_2} = .01225$.

A. Stepwise changes of control parameters

1. *Unknown parameters*

In this section it is assumed that none of the parameters of the model are known and that they have to be inferred at each step of the measurements. The parameters η_1 and η_2 are allowed to change at random in time in a step-like manner, and remain constant between steps. The time interval between steps is approximately 5 periods of firing of the action potential and contains one block of data with 20000 points. Other parameters of the model are fixed at the constant values given in Table I. At each step we infer all parameters of the model assuming their initial values to be zero and their initial dispersion to be infinity as already discussed above. The results of this test are shown in Fig. 8. The inferred values of parameter η_1 are compared with their true values in Fig. 8(a). The time-trace of the unknown coordinate $q_1(t)$ is compared

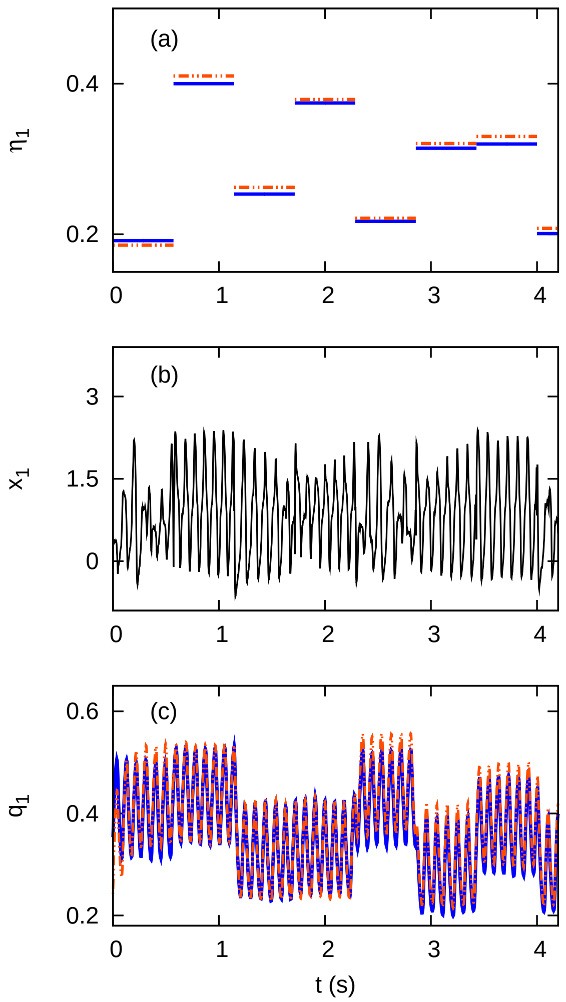

Figure 8: (Color online) Inference of the parameters of two uncoupled FHN systems mixed by the measurement matrix during step-wise changes of η_1 and η_2 and all parameters of the model unknown. (a) The inferred values of η_1 (dashed red lines) are compared with their true values (full blue lines). (b) Measured mixed values of the coordinate $x_1(t)$. (c) Inferred values of the coordinate $q_1(t)$ (red dotted line) are compared with its true values of (blue solid line). The other parameters are fixed at the values given in Table I. The noise amplitude is $\sqrt{d_1} = \sqrt{d_2} = .01225$.

with the corresponding reconstructed time-trace $\tilde{q}_1(t)$ in Fig. 8(c). The latter time-traces were reconstructed as follow. First, the initial coordinates $q_i(t=0)$ and variables $v_i(t)$ were reconstructed using the inferred measurement matrix $\boldsymbol{X}$ and Eqs. (3) and (10). Second, the variable $\tilde{\boldsymbol{q}}(t)$ was reconstructed using Eq. (33) of paper I,

$$
\begin{aligned}
& q_i(t=0) = X_{ij}^{-1}\,\tilde{q}_j(t=0), \\
& y_i(t) = X_{ij}^{-1}\,y_j(t), \\
& \tilde{\boldsymbol{q}}_i(t_k) = \gamma h \sum_{l=0}^{k} e^{(\beta(t_k-t_r))}\boldsymbol{y}(t_r) + e^{-\beta\, t_k}\boldsymbol{q}(0) \\
& \quad - \frac{h\gamma}{2}\left[\boldsymbol{y}(t_k) + e^{-\beta t_k}\boldsymbol{y}(0)\right].
\end{aligned} \tag{17}
$$

It can be seen from the figure that the time resolution of the method is of the order of 500 ms even in the case when *none* of the model parameters are known. As mentioned above, however, the time resolution of the method can be substantially improved by considering the other parameter of the model to be known on the time scale of a few seconds (corresponding to their correlation time, see Sec. II) and tracking in time only the time-varying control parameters η_i.

2. *Tracking control parameters with known dynamics*

We now investigate how fast physiological parameters can be tracked in time. It was shown above (see Sec. III C) that the convergence speed depends on information about the model parameters that is available *a priori*, and that the fastest time resolution can be achieved when all the parameters of the model, except the control parameters η_i, are known. To demonstrate this effect we now assume that η_1 and η_2 change stepwise at random and remain constant between steps as above, but that all other parameters of the model remain fixed at known values. The time interval between steps is now approximately 0.03 s and contains one block of data with 1000 points. The results of Fig. 9 show that the method can track random, step-wise, variations of the control parameters with a time resolution of less then 0.03 s (i.e. smaller by more than two orders of magnitude than in the previous case where all parameters had to be inferred).

B. Continuously varying control parameters with noise

To complete our analysis of the reconstruction of nonstationary dynamics of the physiological model, we now infer smoothly varying parameters η_1 and η_2 with added noise, without knowing any other parameters of the model. The test is performed as follows: (i) all parameters of the model are inferred from the first block (with 30000 points) of stationary dynamics; (ii) for all other blocks of data we use acquired information to fix the model parameters constant at the inferred values, and track in time only variations of the control parameters η_i. Each block of data (except the first one) contains 12000 points and has a time length $t \approx 0.34$ sec. The

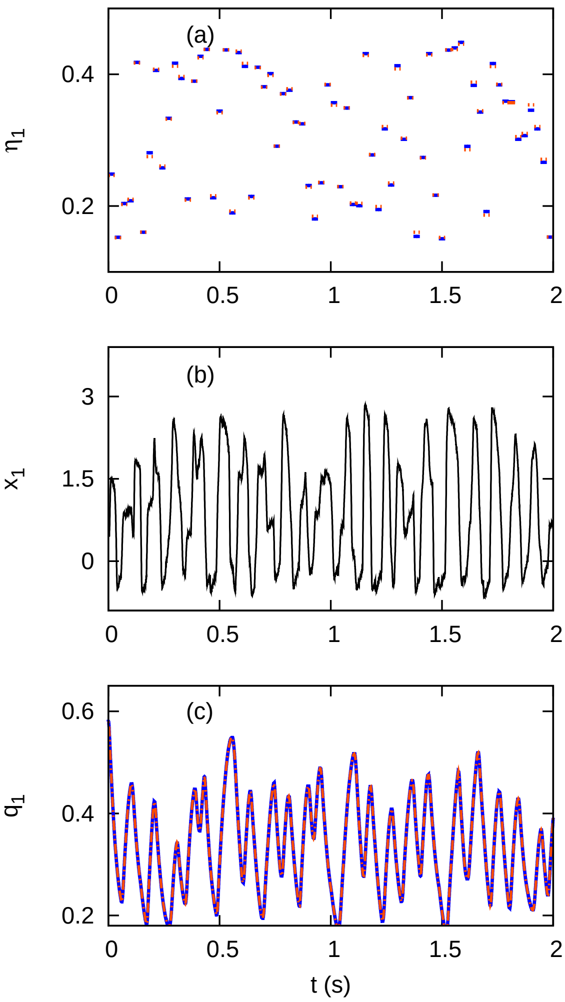

Figure 9: (Color online) Inference of the model parameters of two uncoupled FHN systems mixed by the measurement matrix with step-wise changes of η_1 and η_2 when all other parameters of the system are known. (a) Inferred values η_1 (short elements of red dashed line) are compared with their true values (short elements of full blue line) as a function of time. (b) The time-trace of the measured coordinate $x_1(t)$. (c) The time-trace of the inferred coordinate $\tilde{q}_1(t)$ (red dotted line) is compared with its true value $q_1(t)$ (blue solid line). The values of the other parameters are fixed, as given in Table I. The noise amplitude is $\sqrt{d_1} = \sqrt{d_2} = .01225$.

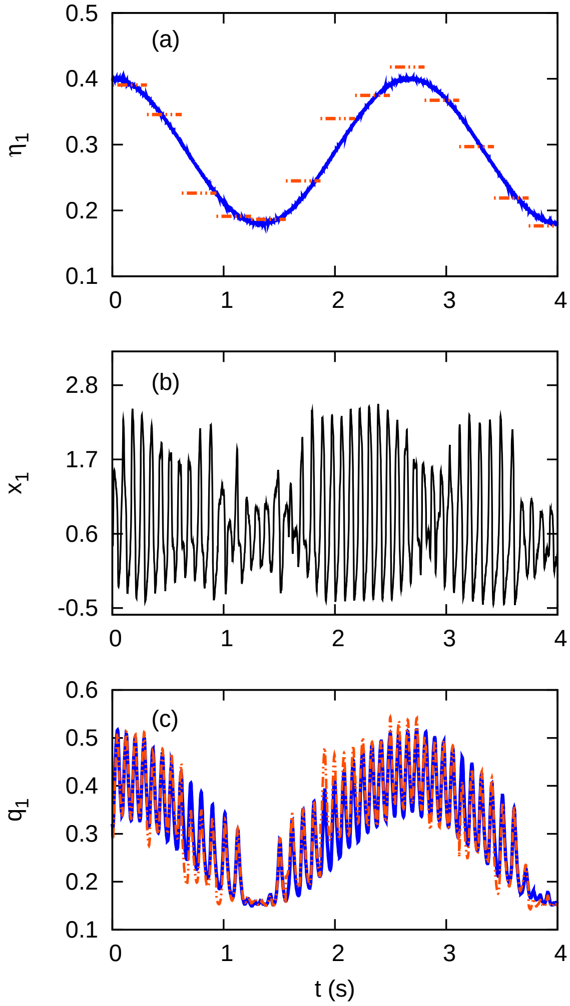

Figure 10: (Color online) Inference of η_1 and η_2, while smoothly varying in the presence of noise. No prior knowledge of the model parameters is assumed. (a) The inferred values of η_1 (dashed red lines) are compared with their true values (full blue lines). (b) The measured time-trace of the mixed coordinate $x_1(t)$. (c) The inferred time-trace of the mixed coordinate $\tilde{q}_1(t)$ (dashed red line) is compared with its true value $q_1(t)$ (full blue line). The values of the other parameters are given in Table I. The noise amplitude is $\sqrt{d_1} = \sqrt{d_2} = .01225$.

time-traces of the unknown variables $q_i(t)$ reconstructed at every step using Eqs. (17) as explained above. The inferred time evolution of the control parameters η_i is compared with its true variation in Fig. 10. It is evident from the figure that the method allows to infer the unknown constant parameters of the model, and then also to use this information to track in time the non-stationary control parameters of the system with a time resolution of the order of 0.3 sec.

V. CONCLUSION

In summary, we have explored the performance of the novel Bayesian inferential framework for non-stationary dynamics that we introduced in Paper I [6] in relation to physiological applications. We did so by modelling a physiological signal as a set of fast variables y_i, mixed by unknown measurement matrix, corresponding to the action potentials of stochastic FHN oscillators. Our goal was to see whether we could track on-line the control parameters η_i of the model, given that these can vary with correlation time $\tau_{cor} \lesssim 500\,\text{ms}$. It was assumed that the slow recovery variables of the FHN oscillators were unavailable for measurement and that the correlation time of all other unknown parameters of the model was of the order of 5 s. We have established that the method dies indeed facilitate allows on-line tracking of η_i with a time resolution < 0.3 sec. This was achieved by embedded the model within a Bayesian learning framework for the more slowly varying parameters with a time resolution < 1 s.

We showed that the time resolution of the method is determined by the eigenvalues of the matrix $\hat{\mathbf{\Xi}}^{-1} = \hat{\mathbf{D}} \otimes \hat{\mathbf{\Phi}}_k^{-1}$, and therefore depends essentially on the choice and scale of the base functions. Note that, while the eigenvalues of $\hat{\mathbf{D}}$ are intrinsic to the system, the choice and scale of the base functions can be controlled by the researcher. Specifically, we demonstrated that by accumulating *a priori* information about slowly-varying model parameters, one can enhance the time resolution of the control parameters by an order of magnitude.

Several limitations of the method should be borne in mind in adapting it to any particular application. As we have already mentioned, fast online applications require that measurement noise be small. In addition, it was assumed that the equations for the hidden variables are linear and deterministic. The latter limitations can be removed, at least partially, by writing the equation for the hidden variables in the more general form $\dot{q} = f(q)+g(y)$, where the homogeneous equation $\dot{q} = f(q)$ is integrable and the nonlinear function of the measurable variable $g(y)$ is arbitrary. One can then proceed in exactly the same way as described in the present paper. Furthermore, the method can be extended to encompass the case of an integrable stochastic differential equation for the hidden variables. To do so, a stochastic integral must be added to the right-hand sides of the equations of reduced dynamics. Finally, the method can be applied to the case in which the dynamics of the system jumps at random between different states, as, for example, in gating dynamics of ion channels. Note, however, that if the different states are characterized by different dynamical models, then the solution of the inference problem can be obtained more generally within the framework of a hybrid probabilistic approach, as will be described in more detail elsewhere. We note that the method is also useful when the low-dimensional dynamics is only a rough approximation to the actual multidimensional complex dynamics of the system. The latter situation is often the case in physiological and aerospace applications [21, 22].

We conclude, therefore (see also [6]), that the results obtained are of broad interdisciplinary interest. They were recently shown to be particularly useful in medical applications [20] and for development of prognostics and diagnostics techniques in aerospace applications [21, 22]. The method can readily be extended to encompass systems with multiplicative and colored noise, and efforts towards these ends are already in progress.

Acknowledgments

We are grateful to the Engineering and Physical Sciences Research Council (UK) and NASA for financial support.

[1] R. Mukkamala and R. J. Cohen, Am. J. Physiol.: Heart. Circ. Physiol. **281**, H2714 (2001).
[2] S. Lu and K. H. Chon, IEEE Trans. on Sig. Proc. **51**, 3020 (2003).
[3] A. B. Schwartz, X. T. Cui, D. J. Weber, and D. W. Moran, Neuron **52**, 205 (2006).
[4] F. Lotte *et al.*, Journal of Neural Engineering R1 (2007).
[5] S. Eyal and S. Akselrod, Meth. of Inform. in Medicine **39**, 118 (2000).
[6] D. G. Luchinsky, V. N. Smelyanskiy, A. Duggento, and P. V. E. McClintock, "Inferential framework for nonstationary dynamics. Part I. Theory", Phys. Rev. E **77**, 061105 (2008).
[7] R. FitzHugh, Biophys. J. **1**, 445 (1961).
[8] J. Nagumo, S. Animoto, and S. Yoshizawa, Proc. Inst. Radio Engineers **50**, 2061 (1962).
[9] A. T. Winfree, *The Geometry of Biological Time* (Springer-Verlag, New York, 1980).
[10] J. Keener and J. Sneyd, *Mathematical Physiology* (Springer-Verlag, New York, ADDRESS, 1998).
[11] E. N. Best, Biophys. J. **27**, 87 (1979).
[12] J. Rogers and A. McCulloch, IEEE Trans. Biomed. Eng. **41**, 743 (1994).
[13] R. R. Aliev and A. V. Panfilov, Journal of Theoretical Biology **181**, 33 (1996).
[14] P. Chen, SIAM J. Math. Anal. **23**, 81 (1992).
[15] O. Berenfeld and S. Abboud, Med. Eng. and Phys. **18**, 615 (1996).
[16] D. Bullock, P. Cisek, and S. Grossberg, Cereb. Cortex **8**, 48 (1998).
[17] S. Rajasekar and M. Lakshmanan, J. Theor. Biol. **166**, 275 (1994).
[18] R. Mannella, Intern. J. Mod. Phys. C **13**, 1177 (2002).
[19] D. M. Bates and D. G. Watts, *Nonlinear Regression and Its Applications* (Wiley, New York, 1988).
[20] D. G. Luchinsky *et al.*, Phys. Rev. E **72**, 021905 (2005).
[21] V. V. Osipov, D. G. Luchinsky, V. N. Smelyanskiy, and D. A. Timucin, *Proc. AIAA/ASME/SAE/ASEE Joint Propulsion Conf. and Exhibit*, *AIAA Conference Proceedings* (AIAA, Cincinnati, OH, 2007), p. 5823.
[22] D. G. Luchinsky *et al.*, *Proc. AIAA Infotech@Aerospace 2007 Conf. and Exhibit*, *AIAA Conference Proceedings* (AIAA, Robnert Park, CA, 2007), p. 2829.